PILOT LINE RESULTS OF N-TYPE IBC CELL PROCESS IN MASS PRODUCTION ENVIRONMENT

N. Guillevin[1], I. Cesar[1], A.R. Burgers[1], P. Venema[2], Z. Wang[3], J.Y. Zhai[3], D. Liu[3]

[1] *Energy research Centre of the Netherlands, P.O.Box 1, 1755 ZG Petten, The Netherlands,*
[2] *Tempress Systems B.V., Radeweg 31, 8171 MD Vaassen, NL*
[3] *Yingli Energy (China) Co., Ltd. 3399 North Chaoyang Avenue, Baoding, China, 071051*

Together with Yingli Solar and Tempress Systems, ECN accelerates the development of the Mercury IBC technology by implementing its low-cost cell process in a mass production environment. The Mercury solar cell concept based on a bifacial IBC cell design with a front floating emitter (FFE) can now be fully processed on Yingli's pilot line. Pilot processing in an industrial environment offers a great opportunity for the Mercury technology to gain in maturity through an effective bottom-up approach. With a cell process using similar specifications as the commercial n-PERT process, the implementation of the Mercury IBC technology went fast reaching cell efficiencies close to 21% in less than a year. The FFE which renders the cell resilient to electrical shading and reduces the demands on feature size, allowing a high tolerance cell processing. This key feature of the Mercury cell concept plays a major role when it comes to high throughput industrial manufacturing up to module level. Before the end of the year, a set of optimisations will be applied to the rear-side diffusion pattern and to the metallisation with the objective the reach cell efficiencies of 22%. Manufacturability aspects, lab performance and the results of piloting the IBC Mercury technology are described in this paper. Further efficiency gain towards 24% based on the use of polysilicon is also discussed in this paper.

Keywords: interdigitated back-contact; n-type silicon; pilot production

1 INTRODUCTION

The recent international technology roadmap for photovoltaics predicts an increasing market share of back-contact module technology and n-type material for the coming decade [1]. This forecast is supported by market trends towards higher performance, lower costs/kWh, and by the interest in improved aesthetics of PV systems. Connected to this forecast, a relatively new trend is the appearance of bifacial modules in the market. With the incentive of developing state-of-the-art photovoltaic technologies for the industry, ECN has designed a low-cost and industrial bifacial n-type Interdigitated Back Contact (IBC) homo-junction solar cell known as the Mercury IBC technology currently implemented in mass production environment.

In contrast with the well-known IBC cells with front surface field (FSF), the ECN's IBC cell technology employs a conductive p+-doped front floating emitter (FFE). A schematic cross-section of the Mercury cell is shown in Figure 1. The FFE, key feature of ECN's Mercury IBC cells, enhances lateral transport properties for minority carriers (holes) at the front. In addition, it induces a "pumping effect" which transports holes from regions above the BSF to the rear emitter. The additional collection pathway limits the effect of electrical shading of the BSF areas at the rear that conventional FSF IBC cells suffer from.

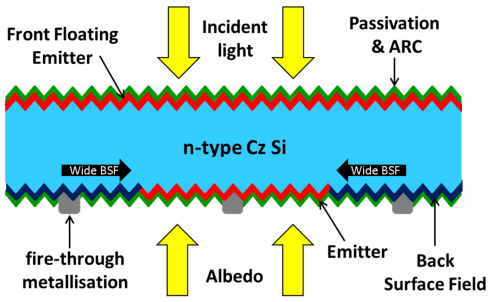

Figure 1. Schematic cross-section of a bifacial Mercury IBC cell. The rear side can receive light, except for where the metallization is present.

With proper tuning of conductance and J_0, the FFE can be applied as an effective means to increase the BSF width with marginal loss in cell performance while assuring process simplification and cost reduction [2].

The integral IBC Mercury solar cell and module concept is currently being piloted in mass production environment at Yingli Solar. This step towards industrialisation is the perfect opportunity for a fast development of the Mercury IBC concept and a precious gain of knowledge on manufacturability of such back-contact solar cell and module technology.

After a review of the manufacturability aspects and lab performance, the pilot line results of the IBC Mercury cell process are discussed. Cell performance progression and pathway to reach the cell efficiency target of 22% at Yingli before the end of 2017 are shown.

Finally, ambitions to raise efficiency of the IBC Mercury cell technology towards 24% keeping an industrial and cost effective process will be discussed.

2 MANUFACTURABILITY AND PERFORMANCE

a. A cost effective industrial process

Despite a different cell architecture, ECN's Mercury IBC process technology remains close to our industrial n-PERT technology in production at Yingli. Similar process equipment as well as process parameters are used without increasing the number of major manufacturing steps making the Mercury process compatible with an industrial scale production and throughput. Cells are processed on commercially available 6 inch n-Cz wafers. The cell structure comprises an interdigitated boron-doped emitter and a phosphorous-doped Back Surface Field (BSF) on the rear-side and a boron-doped FFE on the front-side. Doped regions are created by means of tube diffusion processes and are designed to be suitable for industrial throughput, i.e. lower cycle time and high load density. The FFE and the rear emitter are formed in a single Boron diffusion step. Structuring of the rear-side diffusions is based on conventional screen printing process and does not involve the creation of a gap between the emitter and the BSF. This patterning

approach greatly simplifies processing of the device and reduces manufacturing costs compared to complex and costly high resolution patterning techniques such as lithography or LASER ablation processes. In addition, this approach offers a great flexibility in implementing different diffusion pattern designs and matching metallisation grid designs. Front-side and rear-side surface passivation and anti-reflecting coatings are applied by industrial ALD and PECVD equipment respectively. The metallisation consists of a firing-through Ag paste deposited in a single step, for both emitter and BSF, by screen-printing and features an open grid design suitable for thin wafers and bifacial applications. The currently used metallisation grid design at ECN includes busbars and 62 interconnections pads as shown in figure 2.

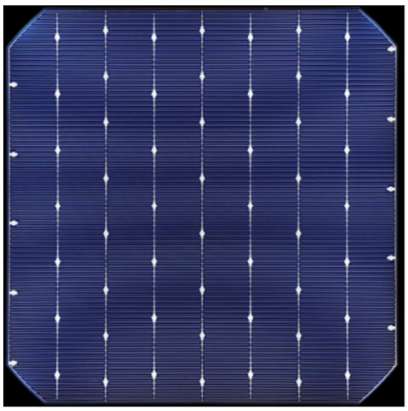

Figure 2. Rear-side grid design of the IBC Mercury cell as processed at ECN.

A major objective in the development of the Mercury IBC technology was to change the market perception that an IBC process is laborious and expensive. Great efforts dedicated to simplify the manufacturing process resulted in placing the process complexity of Mercury cells next to that of p-PERC cells. The process cost, excluding the cost for wafer and silver paste, reached a cost level comparable to that of p-PERC [2]. With an attractive module and system cost, the Mercury IBC technology is ready to enter the market of low-cost PV technology.

Flexibility of the diffusion pattern and metallisation grid designs offers freedom when it comes to the choice of module interconnection technology. Both diffusion and metallisation patterns can be easily modified to be made compatible with many interconnection technologies. Based on the current metallisation grid design which includes interconnection pads, the cells can be readily processed into modules using ECN's foil-based interconnection technology [4-5]. ECN's module manufacturing technology is based on an interconnection foil with integrated conductor layer (e.g. copper or aluminium), on which the cells are electrically contacted using a conductive adhesive. Compared to a tabbed interconnection technology, the interconnection foil allows reduction of the module series resistance by using more interconnect metal (more cross-sectional area) and thereby reduces the cell to module FF loss. Also, the module manufacturing based on integrated back-foil can be done with higher yield and reduced interconnection-process-related stress, allowing use of (much) thinner cells and therefore offering additional cost reduction possibilities. The interconnection technology by itself has also potential for improvement and further cost reduction, as reported in [6]. So far, 2x2 cells IBC Mercury laminates successfully passed damp heat and thermal cycle tests as described by the IEC 61215 standard. The IBC cells that are free of front metallisation give the module an aesthetical appearance as illustrated in figure 3. Based on the same interconnection technology, a first 60-cell module is in preparation to monitor cell-to-module losses.

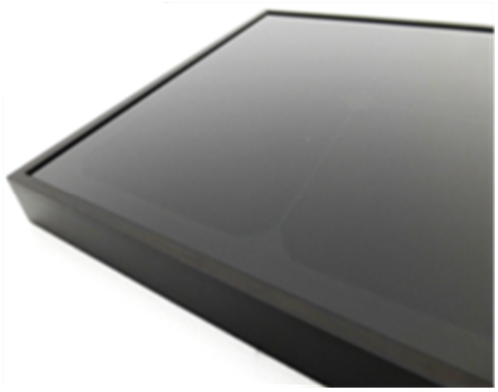

Figure 3. Photographic image of an all-black 2x2 Mercury IBC module

The metallisation grid design can be easily modified to be made compatible with for instance the multi-wire interconnection technology [7]. This alternative type of interconnection will allow the technology to benefit from the full bifaciality potential of the Mercury IBC cells for increased annual energy yield when installed in the field.

b. Cell performance processed on ECN's pilot line

We have been able to steadily increase the efficiency of our cells on ECN's pilot line, and reported our best efficiency to date of 21.1% [2]. The I/V parameters of this cell are listed in Table 1. The I/V parameters were obtained with an in-house measurement using a class AAA solar simulator. The measurement chuck was especially designed for our Mercury cells, with current and voltage probes only contacting the module interconnection points, and a reflective but non-electrically-conductive chuck surface, representative for the situation in a module. The J_{sc} was corrected for spectral mismatch. The measurement was calibrated with a Fraunhofer-ISE-calibrated front-and-rear contact cell measured with a different chuck. Both for calibration and for IBC cell measurements, the chuck surface outside of the cell was masked with black tape, to avoid calibration errors due to variation in the chuck area and chuck reflectance.

Table 1. I-V parameters of the best Mercury IBC cell measured at ECN. Short circuit current is corrected for spectrial mismatch

Area	J_{sc} (mA/cm^2)	V_{oc} (mV)	FF (%)	Eta (%)	Bifaciality factor
239	41.2	653	78.4	21.1	83%

Performance of our Mercury cells can be further improved, in particular in V_{oc} and FF. By improving the rear-side diffusion pattern and metal contact properties that enable smaller contact areas and less recombination, efficiency improvement beyond 22% is within reach.

Work in this direction is being carried out and will be discussed in the next sections.

The bifaciality factor of our Mercury IBC cells was also measured on ECN's I/V tester. To allow a proper rear-side I/V measurement, ribbons were connected to the contact pads of the cell metallisation grid by soldering. Front and rear-side I/V measurements were carried out by contacting the cell to the soldered ribbons. A high bifaciality factor of 83% was measured illustrating the great potential for higher annual energy yield when the cells will be interconnected in a bifacial module configuration.

3 MERCURY IBC OPTIMISED IN MASS PRODUCTION ENVIRONMENT

a. An effective bottom-up technology development

Only a few 6 inch wafer based IBC pilot lines exist in the world and information on the manufacturability of this cell type is scarce because of that. From a long-lasting cooperation with the Chinese PV manufacturer Yingli Solar and with the support of Dutch equipment supplier Tempress, ECN has the chance to implement the cost effective Mercury IBC process in a mass production environment to accelerate development of the technology. This collaboration towards high performance industrial cell and module technology is the perfect opportunity to ease development aiming at reaching a technology readiness level suitable for a successful introduction to the market.

Rapidly after setup of the Mercury IBC pilot line at Yingli, implementation of the IBC cell process started in the third quarter of 2016 as shown in figure 4. In only a quarter of a year, Yingli had processed their first batch of Mercury IBC cells with a top efficiency of 19.3% illustrating the compatibility of ECN's IBC Mercury technology with mass production equipment. After couple of month of process stabilisation, a cell efficiency of 20.5% was reached just before the end of 2016. With this important milestone completed, the consortium could focus on improving further the cell efficiency through a step by step optimisation of the different key design and process aspects.

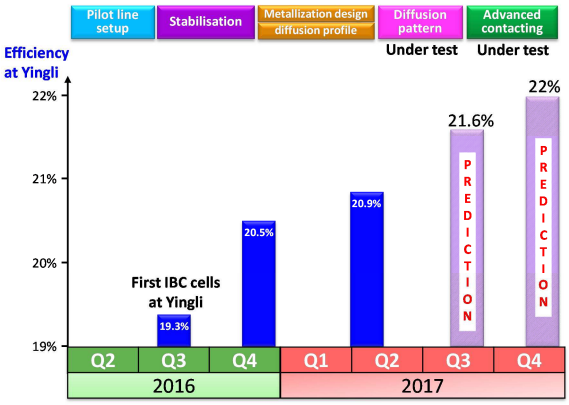

Figure 4. Efficiency progression of the Mercury IBC cells processed in mass production environment

b. Technology optimization – achieved results

All processing is performed on Yingli's PANDA production line offering high throughput pilot process for a fast turnover of experiments. As shown in figure 4, the first quarter of 2017 was dedicated to the metallisation grid design improvement. To evaluate performance of the cells, design of the metallisation grid has to be compatible with the contacting chuck used to measure I/V parameters. In order to process the first measurable batch of IBC cells as early as possible, the metallisation grid was designed to match Yingli's measurement chuck operational at this time which included 31 contact points. This suboptimal design leads to significant fill factor (FF) losses estimated at 1.1% absolute. A new chuck design with 81 contact points became available at Yingli at the beginning of 2017 offering the opportunity to redesign the metallisation grid to reduce resistive losses. The earlier metallisation grid design (from 2016) and current metallisation grid design are shown in figure 5. From modelling, the FF would increase by around 0.7% absolute by increase the number of contact points from 31 to 81, without increasing of the metal paste fraction. The modelled fill factor loss breakdown is shown in table 2.

Figure 5. Mercury IBC former metallisation grid design with 31 contact pads (2016 design, left picture) and current metallisation grid design with 81 contact pads (2017 design, right picture) as processed at Yingli

Table 2. Modelled FF loss breakdown for the 2 different metallisation grid designs featuring 31 and 81 contact pads

Absolute FF loss	31 contact pads	81 contact pads
In metal fingers	0.60%	0.20%
In metal Busbars	0.50%	0.15%
Total FF loss	**1.10%**	**0.35%**

Surface passivation of IBC cells is of high importance, firstly for high J_{sc} due to the long path lengths that minority carriers need to travel before being collected, and secondly to build up a substantial carrier density in order to achieve high V_{oc}. Therefore, in parallel to the metallisation grid design optimisation, emitter, FFE and BSF diffusion profiles were improved for better surface passivation in order to further increase the V_{oc} and J_{sc} of our IBC cells. Improvement of the surface passivation was achieved by reducing dopant concentration at the surface of the three doped layers (FFE, emitter and BSF). In order to keep the overall cell process industrial and cost-effective, the adjustment of the three diffusion profiles is integrated within an already existing process step. Therefore the number of major manufacturing process steps remains the same. Also, the improvement of the dopant profiles consists of a uniform reduction of dopant concentration over the wafer surface. No additional patterning step is involved to create

selectivity in the diffusion profiles commonly used to maintain high dopant concentration under the metal contacts to prevent FF loss. In consequence, this optimisation step is a trade-off between improving surface passivation and maintaining good contact resistance to prevent FF loss.

Thanks to the high throughput of Yingli's pilot line, fast processing of batches of hundreds of cells can be processed improving results statistics. Also, test structures were included in each process run to easily measure valuable parameters such as J_0 of the surface. Three different optimisation levels were tested. For each optimisation level, J_0 surface of the emitter, of the FFE and of the BSF was measured. The J_0 surfaces of the original and most performant doping profiles are reported in table 3.

Table 3. Surface dark saturation current densities (J_0) of the original [D1] and most performant [D3] emitter, FFE and BSF profiles, measured on test structures.

	[D1]	[D3]
Emitter & FFE J_0 surface	65 fA/cm^2	50 fA/cm^2
BSF J_0 surface	290 fA/cm^2	200 fA/cm^2

Means and confidence intervals of the open circuit voltage (V_{oc}) and fill factor (FF) of the IBC cells processed with the three different optimisation levels are shown in figure 6. The experiment is based on batches of more than hundred cells. For each optimisation level of the doping profiles, a firing optimisation was performed to adjust the fire-through contact formation to the new dopant surface concentration. A significant increase of around 6 mV in V_{oc} is reached with the third optimisation level [D3] without FF loss nor J_{sc} loss. This V_{oc} gain is consistent with the J_0 surface reduction of the different diffusions reported in table 3.

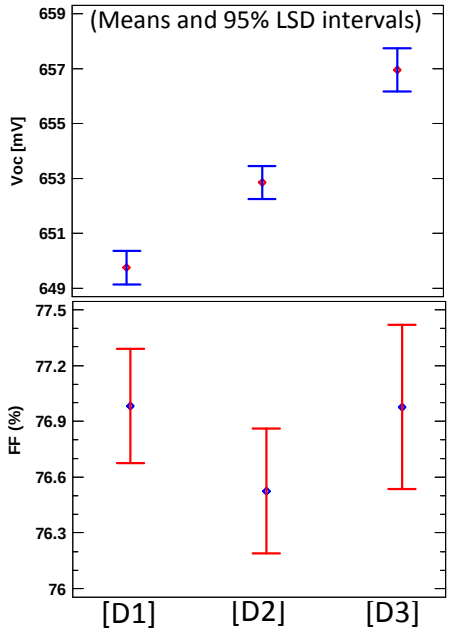

Figure 6. Open circuit voltage (V_{oc}) and fill factor (FF) (means and confidence intervals LSD: Least Significant Difference $p<0.05$) of the IBC cells processed with the three optimisation levels of the doping profiles [D1], [D2] and [D3].

The optimised diffusion profiles were tested together with the new metallisation grid design in a run carried out at Yingli at the beginning of the second quarter of 2017. From this new run, a significant efficiency increase of 0.4% absolute was obtained on the 2016 champion cells with the V_{oc} and FF gain expected from the metallisation design and diffusion process improvements. To confirm I/V measurement accuracy, these champion cells were also measured at ECN. The I/V data comparing the champion cell of 2016 and the champion cell of 2017 are shown in table 4.

Table 4. I/V characteristics of Yingli's champion IBC cells (2016 and 2017) measured at ECN. J_{sc} is corrected for spectral mismatch, cell area=242.8cm2

Date	Cell features	J_{sc} [mA/cm^2]	V_{oc} [mV]	FF [%]	Eta [%]
December 2016	31 contacts [D1] profile	40.4	657	77.4	20.5
April 2017	81 contacts [D3] profile	40.5	663	78.0	20.9

In less than a year, efficiency of 20.9% were reached on 6 inch n-type Cz wafers fully processed at Yingli which demonstrate an effective bottom-up efficiency development in a mass manufacturing environment that is hard to achieve at an R&D facility.

c. Towards 22% efficiency

The current performance of the Mercury IBC cells is currently limited by the open circuit voltage, due to high recombination dominated by the emitter contacts and the heavily doped BSF area. Therefore, reducing both the BSF area and the emitter contact fraction is a route to decrease the recombination in the cell and therefore enhance the cell performance.

Depending on the contact width and the screen printing tolerances, a minimum width of the passivated BSF area is required, which is typically more than 300 µm. In a one-dimensional interdigitated finger design, the only option to reduce the BSF area fraction further is then to increase the emitter width, but this induces large transport losses. Therefore, we reduced the BSF length within the unit cell, and in this way we created "islands" of BSF surrounded by the rear side emitter. Unit cell schematic representations of the standard interdigitated and "BSF islands" diffusion patterns are shown in figure 7. The performance of the "BSF islands" diffusion pattern together with improvement of the FFE passivation has been already reported by ECN on a previous publication [8]. Similar point-contact structures for the diffused areas have been studied before for IBC cells [9]-[10], but in these cases, the BSF islands were mainly created to study the electrical shading reduction benefits. In the Mercury IBC case, electrical shading is not a major issue due to the collecting and transporting front floating emitter. Therefore, the BSF area reduction will mainly improve the passivation of the cell.

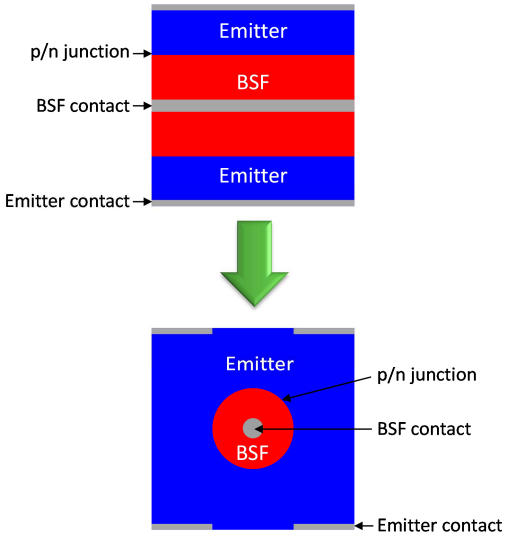

Figure 7. Unit cell schematic representations of the standard interdigitated (top) and "BSF islands" (bottom) diffusion patterns

The "BSF islands" design was tested in the latest ECN's IBC baseline run together with improvement of the FFE passivation. The ECN's IBC baseline run is meant to regularly control ECN's equipment and process stability. The baseline process does not include the latest improvements required to reach efficiencies in the range of the champion cells. Therefore the baseline group reaches average efficiencies around 20.5%. In this test, the baseline reference group is process with an interdigitated diffusion pattern with 37% BSF fraction and 6% emitter metal contact fraction. The "BSF islands" diffusion pattern has 20% BSF fraction and 4% emitter metal contact fraction. As shown in figure 8, the group processed with the "BSF islands" diffusion pattern outperforms the baseline group processed with the standard interdigitated diffusion pattern. The 0.5% absolute efficiency gain obtained thanks to the "BSF islands" diffusion design combined with improved front side passivation is in fair agreement with the simulation results based on Quokka previously reported in [8]. The "BSF islands" diffusion pattern is currently being tested at Yingli.

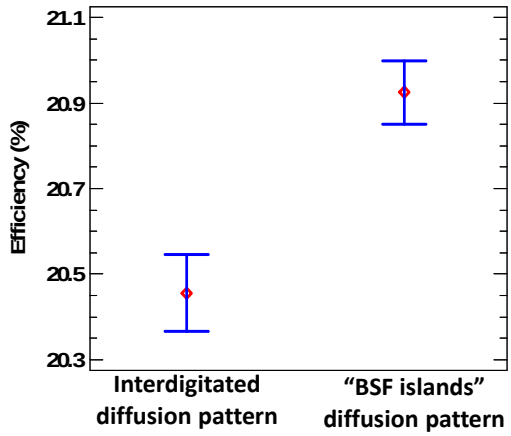

Figure 8. Mercury IBC cell efficiencies results (means and confidence intervals) from the latest ECN's baseline run. The reference group is processed with the interdigitated emitter and BSF diffusion pattern. The test group is processed with the "BSF islands" diffusion pattern.

Short circuit current of Yingli's IBC cells can yet be further improved by simple tuning of the SiNx refractive index to match performance of ECN's champion IBC cells. In combination with the 0.5% absolute efficiency gain from "BSF islands" diffusion pattern, Mercury IBC cells are predicted to reach efficiencies of 21.6% before the end of the third quarter of 2017 as marked in figure 4.

Additional gains in open circuit voltage and fill factor are required to reach the 22% efficiency target before the end of the year. As mentioned earlier, the current Mercury cell process involves screen-printed firing through (FT) metallization. The contacting mechanism of FT metallization is a trade-off between the depth to which the paste has to etch into the doped silicon to obtain contact resistance as low as possible and the recombination resulting from the etching into the diffusion. Current FT pastes tested on our Mercury IBC cells do not allow contact resistances below 5 mOhm.cm^2. A commercial screen printable non-fire through (NFT) metal paste was recently tested at ECN as alternative to conventional FT pastes. Contact resistance as low as 0.5 mOhm.cm^2 was measured on test structures processed with the NFT paste without increasing recombination at the contacts compared to conventional FT paste. Based on these results, the NFT paste will offer the opportunity to further reduce contact area for additional V_{oc} increase while improving the cell fill factor. Efficiency gain potential was simulated with the 2D modelling program Quokka based on Yingli efficiencies. Simulation inputs are shown in table 5 and simulation results are summarized in the table 6.

As predicted by the simulation run 3, thanks to its excellent contacting abilities, the NFT paste allows a V_{oc} increase of 4mV and a 1% absolute FF gain while reducing further the contact area by 1%. Combined with the "BSF islands" design, the used of the screen printable NFT paste will allow efficiency of the Mercury cells to reach 22%.

Table 5. Inputs parameters used in Quokka 2D modelling program

Simulation runs	Diffusion pattern & BSF fraction	Emitter contact area	Contact resistance [mΩ.cm^2]
1	Interdigitated 37% BSF	6%	5
2	BSF islands 20% BSF	4%	5
3	BSF islands 20% BSF	3%	0.5

Table 6. Output I/V parameters obtained from Quokka 2D modelling program based on inputs listed in table 6. J_{sc} increase of run 2 and 3 are related to the front SiNx optical properties optimisation.

Simulation runs	J_{sc} [mA/cm^2]	V_{oc} [mV]	FF [%]	Eta [%]
1	40.5	663	78	20.9
2	41.2	671	78	21.6
3	41.2	675	79	22.0

Implementation of the NFT metallisation process will shortly begin at Yingli with the objective to reach 22% before the end of 2017.

4 BEYOND 22% EFFICIENT MERCRY IBC CELLS

As discussed previously, the performance of our Mercury IBC cells is currently limited by recombination at doped surfaces and at the metal contacts. Carrier-selective contacts based on the combination of a tunnel oxide and doped polysilicon (poly-Si) layer are therefore of a great interest to further reduce contact recombination and increase cell performance. Passivating contacts based on polysilicon are currently studied at ECN for the so-called PERPoly (Passivated Emitter Rear PolySilicon) solar cell concept [11]. Excellent surface and contact passivation quality of p and n doped poly-Si was recently obtained at ECN. To keep the cell process industrial and cost-effective, ECN focuses on screen printed firing through metallisation process for which contact properties to the poly-Si doped layers was also tested. Table 7 summarizes the dark saturation current density J_0 measured on test structures of contacted (J_0,c) and not contacted (J_0,nc) poly-Si layers for both n- and p-type diffusions with a sheet resistance of respectively 60 Ohm/sq and 200 Ohm/sq. Firing-through metallisation contact resistance (R_{co}) measured on test structures are also reported in table 7.

Table 7. Passivation and contact properties of n- and p-doped poly-Si layers processed at ECN as measured on test structures.

parameters	Units	n doped poly-Si	n doped poly-Si
R_{sheet}	[Ω/sq]	60	200
J_0,c	[fA/cm^2]	200	500
J_0,nc	[fA/cm^2]	5	15
R_{co}	[mΩcm^2]	2	2

Based on these results, several IBC cell architectures were modelled using the Quokka 2D simulation program. Schematic cross sections of the cell architectures simulated are summarized in figure 9. The first study case involves an hybrid poly-Si IBC cell consisting of a conventional Mercury IBC cell with n-doped poly-Si as BSF. The second IBC cell architecture modelled features a full poly-Si rear-side with interdigitated n- and p- doped poly-Si emitter and BSF regions. In the two first study cases, the firing-through metal fingers are 80 microns wide. Finally the third study case is similar to the second study case with interdigitated n- and p- doped poly-Si at the rear-side but the firing-through metal fingers are set to a width of 40 microns. In all study cases, the front side remains the standard p-doped FFE homojunction specific to the Mercury IBC cells.

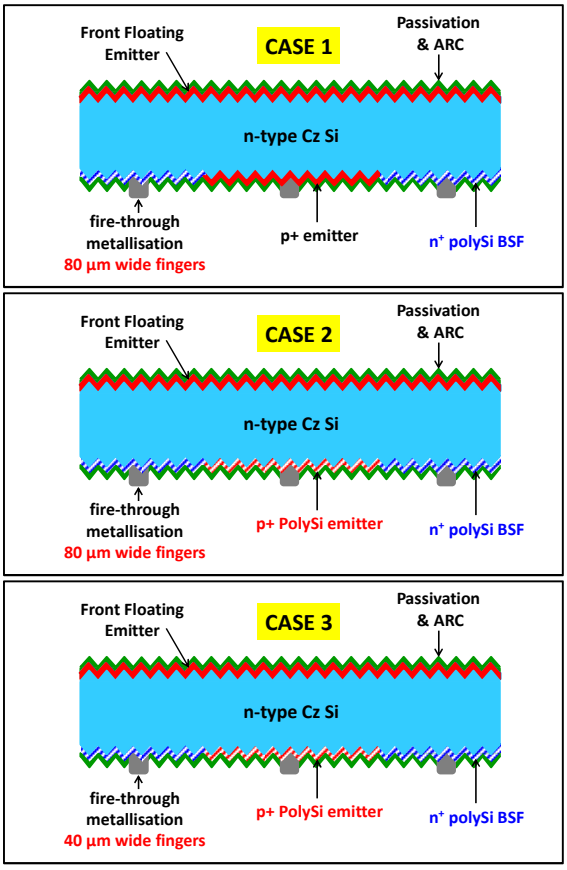

Figure 9. Schematic cross-section of the Mercury IBC cells modelled in Quokka.

Results of the modelling are presented in figure 10 under the form of efficiency contour plots. Efficiency responses are drawn as a function of emitter and BSF half widths. For each contour plot, a red dot indicates the maximum efficiency point with the associated emitter and BSF width. For each study case, a wafer resistivity of 9 Ohm.cm and a bulk lifetime of 2 milliseconds are set as input parameters.

The efficiency contour plot resulting from the simulation of the hybrid poly-Si IBC cell (case 1) shows a maximum efficiency at 22.7% with a wide BSF of 700 microns and a wide emitter of 620 microns as optimum. From the efficiency contour plot of the second case, an almost 1% absolute increase on the maximum efficiency is predicted by the modelling. With a BSF of 560 microns width and an emitter of 600 microns width, a peak efficiency of 23.5% is within reach according to the model predictions. Finally, by reducing metal finger width by half and choosing for narrower BSF and emitter (340 microns and 460 microns respectively) a maximum efficiency of 23.7% is predicted by the modelling. With a 2-3% lower metal fraction compared to the cell structures studied in the two first cases, the cell structure studied in the third case will benefit from an increase bifaciality factor in addition to higher front-side efficiency potential.

The cell design specifications such as emitter and BSF width predicted by the modelling to reach the highest efficiencies remain compatible with high throughput industrial processes such as screen printing.

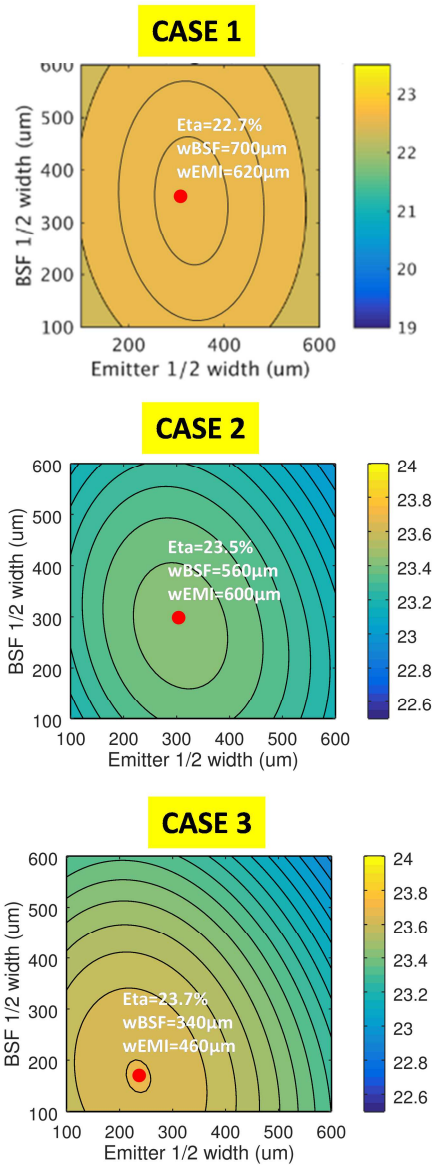

Figure 10. Efficicency contour plots as a function of BSF and emitter half width . These 3 contour plots are the resutls of Quokka 2D simulation for the 3 different IBC architectures showed in figure 9.

5 CONCLUSION

ECN recently teamed up with industry to accelerate the development of its integral bifacial solar cell and module concept based on an interdigitated back-contact cell structure with a front floating emitter: the Mercury IBC technology. Engineered based on a highly tolerant cell process at a cost level of a p-PERC cell, the Mercury IBC technology is currently being piloted on Yingli's production line which offers an ideal environment to bring the concept to high technology readiness level, usually hard to achieve at an R&D facility. The implementation of the process in mass production environment took only a quarter of a year and efficiencies of 20.9% were reached in less than a year. This fast progress illustrated the compatibility of the ECN's IBC Mercury process flow with mass production and shows the high potential for rapid improvements. Based on optimisation of the diffusion pattern and improved metallisation contact scheme, Mercury cells with efficiency of 22% are expected to be manufactured at Yingli by the end of the year. Further efficiency improvement towards 24% become possible when involving passivated contacts as already developed by ECN for the PerPoly cell concept.

With such efficiencies, a high bifaciality factor of 83% and a flexible choice of module interconnection methods, the ECN's IBC Mercury technology clearly becomes a remarkable competitor on the photovoltaic market.

6 ACKNOWLEDGEMENTS

ECN acknowledges the cooperation with Tempress Systems and Yingli solar.

7 REFERENCES

[1] http://www.itrpv.net/Reports/Downloads/ - ITRPV Eighth Edition 2017- Maturity Report 20170906.pdf – page 36

[2] Ilkay Cesar et al., "Enablers for IBC: integral cell and module development and implementation in PV industry", *7th International Conference on Silicon Photovoltaics, SiliconPV 2017.*

[4] Bennett IJ, Eerenstein W, Rosca V. Reducing the cost of back-contact module technology. *Energy Procedia 2013; 38:329-33.*

[5] Bende EE, Van Aken BB. The effect of reduced silver paste consumption on the cost per wp for tab-based modules and conductive-foil based modules. *Energy Procedia 2015;67:163-74.*

[6] Goris MJAA, Kikkert BWJ, Kroon JM, Rozema K, Bennett IJ, Verlaak J. Production of low cost back contact based PV modules, *32nd European Photovoltaic Solar Energy Conference, Munich, Germany, p. 99-104, 2016.*

[7] Johann Walter et al, Multi-wire Interconnection of Busbar-free Solar Cells, *Energy Procedia Volume 55, 2014, Pages 380-388*

[8] A. Mewe, BSF islands for reduced recombination in IBC cells, *IEEE PVSEC-44, Washington DC, June 25-30 2017*

[9] C. Reichel, F. Granek, M. Hermle and S. W. Glunz, "Back-contacted silicon solar cells with insulating thin films", *NPV workshop, 2011*

[10] J. Haschke, N. Mingirulli, and B. Rech, "Progress in point contacted rear silicon heterojunction solar cells", *Energy Procedia 27, 2012, p. 116*

[11] M. Stodolny, Material properties of LPCVD Processed n-type Polysilicon Passivating Contacts and its Application in PERPoly Industrial Bifacial Solar Cells, *7th International Conference on Silicon Photovoltaics, SiliconPV 2017*